A Pragmatic Optimization of Axial Stack-Radial Passive Magnetic Bearings

K. P. Lijesh
Rotor Dynamics Laboratory,
Department of Mechanical Engineering,
National Institute of Technology Karnataka,
Surathkal 575025, India
e-mail: lijesh_mech@yahoo.co.in

Mrityunjay Doddamani
Rotor Dynamics Laboratory,
Department of Mechanical Engineering,
National Institute of Technology Karnataka,
Surathkal 575025, India
e-mail: mrdoddamani@nitk.edu.in

S. I. Bekinal
Department of Mechanical Engineering,
KLS Gogte Institute of Technology,
Belagavi 590008, Karnataka, India
e-mail: sibekinal@git.edu

Passive magnetic bearing's (PMB) adaptability for both lower and higher speed applications demands detailed and critical analysis of design, performance optimization, and manufacturability. Optimization techniques for stacked PMB published in recent past are less accurate with respect to complete optimum solution. In this context, the present work deals with a pragmatic optimization of axially stacked PMBs for the maximum radial load using three-dimensional (3D) equations. Optimization for three different PMB configurations, monolithic, conventional, and rotational magnetized direction (RMD), is presented based on the constraints, constants, and bounds of the dimensions obtained from published literature. Further, to assist the designers, equations to estimate the mean radius and clearance being crucial parameters are provided for the given axial length and outer radius of the stator with the objective of achieving maximum load-carrying capacity. A comparison of the load-carrying capacity of conventional stacked PMB using the proposed equation with the equation provided in literature is compared. Finally, effectiveness of the proposed pragmatic optimization technique is demonstrated by analyzing three examples with reference to available literature. [DOI: 10.1115/1.4037847]

Introduction

Passive magnetic bearings (PMBs) developed from high remanent magnetic materials are considered to be the ideal maintenance free bearings, as they can be operated at high rotational speed without contact and lubricant [1,2]. A monolithic repulsive type PMB (Fig. 1(*a*)) consists of a rotor ring magnet positioned inside another stator ring magnet. In this configuration, polarizations of the rotor and stator magnets are same resulting in axially polarized magnets which are preferred due to availability and economics involved [3]. However, the load-carrying capacity of these PMB is lower and can be improved by stacking number of rings in the axial direction [4,5]. Stacking of rings is achieved in two different ways: (i) conventional (back to back) and (ii) rotational magnetized direction (RMD) [6]. PMB configurations are presented in Fig. 1. Conventional configuration (Fig. 1(*b*)) is materialized by arranging axial/radial polarized ring magnets, back to back, whereas both radially and axially polarized ring magnets are used to achieve RMD as shown in Fig. 1(*c*).

The force exerted on rotor by stator in stacked PMBs depends on number of stacks, bearing dimensions, and strength of the magnetic material [7]. Hence, it is essential to optimize force-dependent variables for maximizing load-carrying capacity prior to the development of stacked PMBs. Design of PMBs with two-dimensional (2D) analytical equations for estimating radial/axial force using is presented by many researchers [4,5,7,8]. In 2D equations, the cylindrical PMBs are considered as infinite parallelepiped magnets instead of cylinders. This consideration neglects the curvature of PMB and due to which the accuracy of the estimated values by 2D equation reduces with increase in radius of PMB [9] and cannot estimate the values of force with change of eccentricity. Therefore, in the present work, a three-dimensional (3D) equation is used to estimate the values of force. Lijesh and Hirani [7] modified 2D equations of Yonnet et al. [5] by incorporating effect of eccentricity and different rotor and stator widths on force through statistical analysis. However, their equation is valid only for few dimension ranges of PMBs. Recently, Van et al. [10] carried out optimization for all the topologies of a PM thrust bearing using 2D analytical equations, for maximizing force and stiffness. Nevertheless, their optimization was lacking completeness, as they have considered equal radial thickness of the rotor and stator magnets. Moser et al. [8] performed optimization using finite element analysis on the conventional stacked PMB for the maximum radial stiffness for a given control volume and provided set of equation to estimate the parameters of the conventional stacked PMB. However, discrete type of optimization is followed requiring more computational time and the equation is valid only if the ratio of clearance to outer radius of rotor is between 0.01 and 0.06. Using 3D numerical equations, Bekinal et al. [11] performed discrete optimization on conventional stacked PMBs for maximizing thrust load and stiffness. From the foregoing literature, the following observations are made:

(1) Complete optimization has not been performed on both types of stacked PMBs.
(2) Optimization for RMD stacked radial PMB has not been carried out.
(3) Complete optimizations have been performed for thrust bearing considering equal radial thickness of rotor and stator magnets.

These observations necessitate the authors to perform complete optimization on both types of stacked PMBs for radial load and understand the variation in the dimensions of PMBs for achieving maximum load. Thus, the objectives of the present work are:

(i) To perform a complete optimization by interior trust region optimization method on monolayer and both types of stacked PMBs for achieving maximum radial load. The optimization will be performed considering constant axial length of PMBs with different widths of stacked rings based on number of stacking. Three-dimensional Coulombian equations [12] are adopted for this. To define the constraints, constants, and bounds for the optimization, the dimensions of the PMBs from ten different literatures (inner and outer radii rotor and stator, the axial length of rotor and stator, axial offset, and clearance) [2,3,6,12–18] are considered. In the present work, optimization is performed by considering: inner radius of rotor means radius, clearance, axial offset, and axial length of PMB as variables and the outer radius of the PMB is considered as constant. The variation in the dimension of PMBs is studied.
(ii) To demonstrate the effect of different radial thicknesses of rotor and stator magnets, optimization is repeated for the equal radial thickness of the stator and rotor magnets. The

Contributed by the Tribology Division of ASME for publication in the Journal of Tribology. Manuscript received March 14, 2017; final manuscript received August 26, 2017; published online October 12, 2017. Assoc. Editor: Daejong Kim.

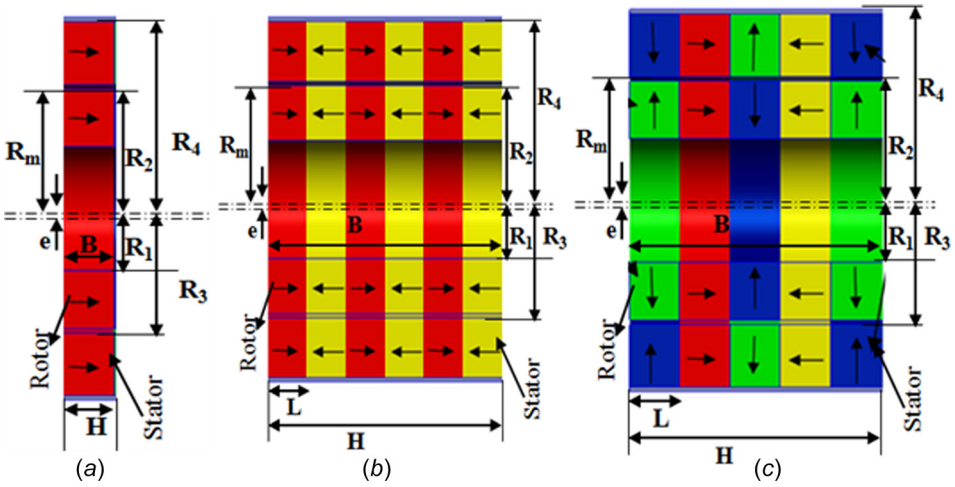

Fig. 1 Configurations of PMB: (*a*) monolithic, (*b*) conventional, and (*c*) RMD

results obtained are compared with the outcome of first objective.

(iii) To provide equations for estimating mean radius and clearance for achieving maximum load for all the configurations. This will allow researchers to design the stacked PMBs in single iterations, rather following trial and error method to find the dimension of PMBs providing maximum load. The radial load for conventional stacking obtained from the proposed equation and equation provided by Moser et al. [8] will be compared.

(iv) To validate and demonstrate the effectiveness of the present approach, dimensions of stacked PMBs from three different published literatures are considered and results will be presented in the findings.

Mathematical Modeling

Three-dimensional Coulombian equations used for estimating the radial load in (i) configuration 1: monolayer PMB (Fig. 1(*a*)), (ii) configuration 2: conventional back to back PMB (Fig. 1(*b*)), and (iii) configuration 3: RMD (Fig. 2(*c*)) PMBs have already been discussed in Refs. [6], [8], [9], [11], [12], [14–16], and [19]. Therefore in the Optimization section focus will be laid in providing the details of the optimization method along with their bounds and constants. The radial load estimated in the present work is sum of both static and dynamic load.

Mathematical Modeling of Configuration 1. The vertical (radial) force exerted by two axially polarized full ring magnets estimated by 3D Colombian approach is presented in the below equation:

$$F_{y,a} = \frac{\mathrm{Br}_1 \mathrm{Br}_2}{4\pi\mu_0}\left(R(z_a) + R(z_a + H - B) + R(z_a + H) + R(z_a - B)\right) \tag{1}$$

where $R(\alpha)$ is given by

$$R(\alpha) = \int_{\theta_3}^{\theta_4}\int_{\theta_1}^{\theta_2}\int_{R_3}^{R_4}\int_{R_1}^{R_2}\left[\frac{\left(e + r_{12}\cos(\theta) - r_{34}\cos(\theta')\right)r_{12}r_{34}}{\left(r_{12}^2 + r_{34}^2 + e^2 - 2r_{12}r_{34}\cos(\theta - \theta') + 2e\left(r_{12}\cos(\theta) - r_{34}\cos(\theta')\right) + (\alpha)^2\right)^{1.5}} dr_{12}dr_{34}d\theta d\theta'\right] \tag{2}$$

where $F_{y,a}$ is the force in Y direction, R_1 and R_2 are the inner and outer radii of the rotor magnet, and R_3 and R_4 are the inner and outer radii of the stator magnet, respectively, as described in Fig. 2(*a*). Eccentricity is represented by e, between the rotor and stator magnet, and H and B are the axial lengths of the stator and rotor magnets, respectively. The value of θ varies from $\theta_1 = 0$ and $\theta_2 = 2\pi$ for full ring rotor magnet and $\theta_3 = 0$ and $\theta_4 = 2\pi$ for a full ring stator magnet. Br1 and Br2 are the values of magnetic remanence. In the present work, the four integrations in Eq. (1) have been solved using trapezoidal numerical integration technique in MATLAB software. The detail of solving the above equation is presented in Ref. [14].

Mathematical Modeling of Configurations 2 and 3. The 3D Coulombian equation used for configurations 2 and 3 is presented in Eqs. (3) and (4), respectively,

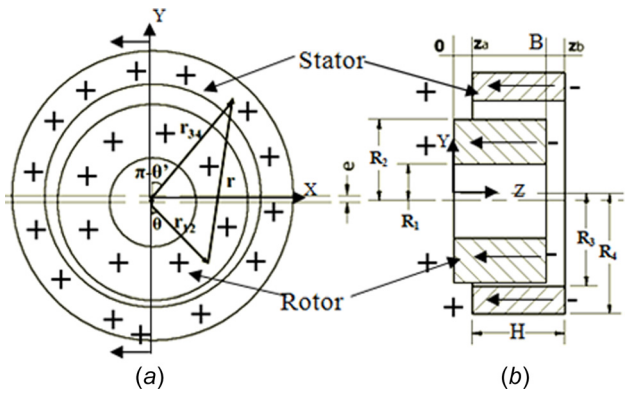

Fig. 2 Configuration 1: coordinates of magnetic bearing. (*a*) Front view and (*b*) sectional side view.

$$F_{y,\mathrm{CON}} = \sum\left(\sum_{j=1}^{k} F_{y,a,j}\right) \tag{3}$$

$$F_{y,\mathrm{RMD}} = \sum\left(\sum_{j=1}^{k} F_{y,a,i,j} + \sum_{j=1}^{m} F_{y,p,i,j}\right) \tag{4}$$

where k is the number of pairs of axially polarized ring magnets and m is the number of pairs of perpendicularly polarized ring magnets in RMD configuration. The radial force generated in a pair of perpendicularly magnetized rings is given by Eq. (5). The details of solving Eqs. (3) and (4) are discussed in Ref. [19]

$$F_{y,p} = \frac{\mathrm{Br}_1 \mathrm{Br}_2}{4\pi\mu_0}\left(A(z_a,R_1) - A(z_a+H,R_1) - A(z_a,R_2) + R(z_a+H,R_2)\right) \tag{5}$$

where

$$A(z_a,R_1) = \int_0^{2\pi}\int_0^{2\pi}\int_0^{L}\int_{R_3}^{R_4} \frac{\left(e + R_1\cos(\theta) - r_{34}\cos(\theta')\right)}{\left(R_1^2 + r_{34}^2 + e^2 - 2R_1 r_{34}\cos(\theta-\theta') + 2e\left(R_1\cos(\theta) - r_{34}\cos(\theta')\right) + (z_a - z_{34})^2\right)} dr_{34}dz_{ab}d\theta d\theta' \tag{6}$$

These equations are utilized to perform optimization.

Optimization

In the present work, inner radius of the rotor (R_1), axial length of the rotor (H), clearance (C), axial offset (z_0), and mean radius (R_m) are considered as variables, while the outer radius of the stator (R_4) magnet is kept constant. The value of R_4 is fixed for proper convergence of optimization results and to overcome the difficulties in developing larger ring magnets. The optimization is performed for a single value of eccentricity ratio ($\varepsilon = e/C = 0.9$) and remanence of rotor and stator magnets is taken as 1 T. The value of eccentricity is set to 0.9 because as even slight contact in magnet asperities causes demagnetization of magnet and damage to magnets. In the present work, the bounds and dimensions of PMBs are extracted from most relevant available literature [2,3,6,12–18], which are used for the optimization approach adopted in the present work. Bound values used in the present work are: $R_1 = 0.002$–0.022 m, $H = 0.003$–0.055 m, $C = 0.0005$–0.01 m, and $z_0 = 0$–0.001. Minimum thickness of magnet from strength perspective is taken as 0.003 m. The value of R_4 is fixed as 0.065 m for the reasons explained earlier. Optimization is performed with the constraint as presented in Eq. (7)

$$R_4 - R_m - 0.5C > 0.003 \tag{7}$$

The finalized constraints, bounds, and constant considered for the optimization in the present work are as follows:

Constraints

$$R_m = \frac{R_2 + R_3}{2} \tag{8}$$

$$R_4 - R_m - 0.5C > 0.003\,m \tag{9}$$

$$\text{bounds} : [H,\ R_1,\ R_m,\ C,\ z_0]$$

$$\text{minimum bound} = [0.003, 0.002, R_1 + 0.003, 0.0001, 0]$$

$$\text{maximum bound} = [0.055, 0.022, R_4 - 0.003, 0.01, 0.0011]$$

constants

$$R_4 = 0.065, \quad \mathrm{Br}_1 = \mathrm{Br}_2 = 1\ \mathrm{T}, \quad \varepsilon = 0.9$$

Optimization is carried out in MATLAB using *fmincon* minimization function and interior-region method for objective function. This method has proved to be very successful in solving large linear programming and nonlinear problems [20], hence adopted in the present work.

Result and Discussion

The first phase of optimization is carried out for maximum load with given constraints, constants, and bounds and to study the parametric variation. Optimization is performed on configuration 1 and the attained objective function values for a different number of iterations are plotted in Fig. 3. From this figure, it can be observed that the maximum value of the objective function is, −245 N. Negative sign implies minimization of the objective function. In other words, a monolayer PMB having $R_4 = 0.065$ m can have a maximum load-carrying capacity of 245 N. Estimated dimensions of the bearing are listed in Table 1. From these optimized results, the following observations are noted:

(i) Values of H and C are maximum.
(ii) Values of z_0 and R_1 are minimum.
(iii) Magnitude of R_m is found to be intermittent and the radial thickness of rotor magnet (0.0463 m) to stator magnet (0.0267 m) is 1.73, indicating, magnets thickness differs.

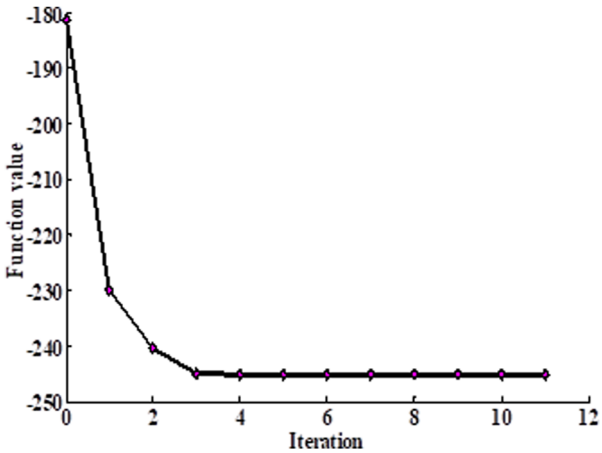

Fig. 3 Convergence of the function value

Table 1 Optimization results of configuration 1

n	F (N)	H (m)	R_m (m)	C (m)	z_0 (m)	R_1 (m)	Vol (m^3)
1	245	0.055	0.0433	0.01	0	0.002	0.019129

Table 2 Optimization results of configuration 2

n	F (N)	H (m)	L (m)	R_m (m)	C (m)	z_0 (m)	R_1 (m)	Vol (m^3)
2	440	0.055	0.0275	0.0443	0.0093	0	0.002	0.019222
3	600	0.055	0.0183	0.0463	0.0077	0	0.002	0.019366
4	688	0.055	0.0138	0.0481	0.0066	0	0.002	0.019559
5	743	0.055	0.0110	0.0496	0.0056	0	0.002	0.019702
6	792	0.055	0.0092	0.0508	0.0049	0	0.002	0.019836
7	829.5	0.055	0.0079	0.0519	0.0043	0	0.002	0.019969
8	861.6	0.055	0.0069	0.0526	0.0039	0	0.002	0.020049
9	888.3	0.055	0.0061	0.0531	0.0036	0	0.002	0.020103
10	910	0.055	0.0055	0.0538	0.0033	0	0.002	0.020205
12	960	0.055	0.0046	0.0549	0.0028	0	0.002	0.020361

Table 3 Optimization results of configuration 3

n	F (N)	H (m)	L (m)	R_m (m)	C (m)	z_0 (m)	R_1 (m)	Vol (m^3)
2	993	0.055	0.0275	0.0581	0.0093	0	0.002	0.001046
3	1369	0.055	0.0183	0.06	0.0077	0	0.002	0.001046
4	1584	0.055	0.0138	0.064	0.0066	0	0.002	0.001048
5	1728	0.055	0.0110	0.069	0.0056	0	0.002	0.001049
6	1807	0.055	0.0092	0.0731	0.0049	0	0.002	0.001053
7	1902	0.055	0.0079	0.0745	0.0043	0	0.002	0.001077
8	1956	0.055	0.0069	0.0756	0.0039	0	0.002	0.001093
9	2007	0.055	0.0061	0.0764	0.0036	0	0.002	0.001110
10	2045	0.055	0.0055	0.0769	0.0033	0	0.002	0.001122
12	2104	0.055	0.0046	0.0772	0.0028	0	0.002	0.001132

Optimization is extended further to configuration 2 (conventional stacking). In this case, Eq. (3) is used as the objective function and the number of stacking n is varied from 2 to 12. The obtained values of maximum load (F), total length of stacking, length of each stacking (L), mean radius (R_m), clearance (C), axial offset (z_0), inner radius of rotor (R_1), and total volume (vol) after optimization are presented in Table 2. The variation in maximum load and attained volume, with respect to a number of stacking, is presented in Fig. 4(*a*). Similarly, the variation in R_m and C values with respect to number of stacking is graphed in Fig. 4(*b*).

From Table 2 and Fig. 4, the following observations are derived:

(i) For attaining maximum load, the values of z_0 and R_1 have to be minimum.
(ii) Value of L has to be maximum.
(iii) Volume increased with n though marginally (5.5%).
(iv) The value of R_m increases and C decreases with increase in n as shown in Fig. 4(*b*).

In the case of configuration 3 (RMD staked arrangement) optimization, Eq. (4) is utilized as the objective function with n varying from 2 to 12. Obtained results are tabulated in Table 3 and the parametric variations are presented in Fig. 5.

From Table 2 and Fig. 5, it can be observed that similar trend is exhibited by the variables R, C, and H as in configuration 2. The increase in volume is estimated to be 6%. Further comparing the load-carrying capacity of configurations 2 and 3 (Tables 2 and 3), it is noted that configuration 3 (RMD) is able to sustain higher loads as compared to configuration 2 (conventional arrangement).

To understand the effectiveness of a pragmatic optimization, the second phase of optimization is performed by considering the equal radial thickness of rotor and stator magnets, i.e., $(R_4-R_3)=(R_2-R_1)$ and the results are compared with earlier ones. The obtained maximum force for configurations 2 and 3 is plotted along with the results of pragmatic optimization in Fig. 6. From this figure, the following inferences are drawn:

(i) The radial load estimated using the pragmatic optimization is higher than the load estimated by considering the equal radial thickness of rotor and stator magnets.
(ii) Reduction in load-carrying capacity is noted for $n>6$ and $n>7$ in configurations 2 and 3, respectively. In the case of pragmatic optimization, the values of radial load increased with increase in n.

It is clearly evident from the above discussion that, in optimization approaches, higher load-carrying capacity is achieved by taking into account different radial thicknesses of rotor and stator magnets instead of equal thicknesses.

Determination of Coefficients for Optimum Load. Selection of bearing dimensions is very crucial for higher load sustainability as seen from earlier discussions. Optimization approach adopted is performed further, for maintaining $R_4=0.065$ m. Behavior of the bearing dimensions, R_m, and C, with respect to L for different R_4 is analyzed and equations are provided herein based on their variation. R_m and C variations with respect to L for configurations 2 and 3 are presented earlier in Figs. 4(*b*) and 5(*b*). From these figures, it can be observed that the mean radius (R_m) increases and clearance (C) reduces with stacking length (L).

The variation of R_m with respect to L and C is plotted in Figs. 7(*a*) and 7(*b*), respectively. From these graphs, the equation relating R_m-L and R_m-C is provided in Eqs. (10) and (11), respectively,

$$R_L = 0.029\ L^{-1.12} \tag{10}$$

$$R_C = 0.024\ L^{-1.21} + 3.14 \tag{11}$$

Optimization is repeated for $R_4=0.055$ m, 0.045 m, and 0.035 m to analyze the influence of variations in dimension for achieving optimum load. The obtained optimum force for varying

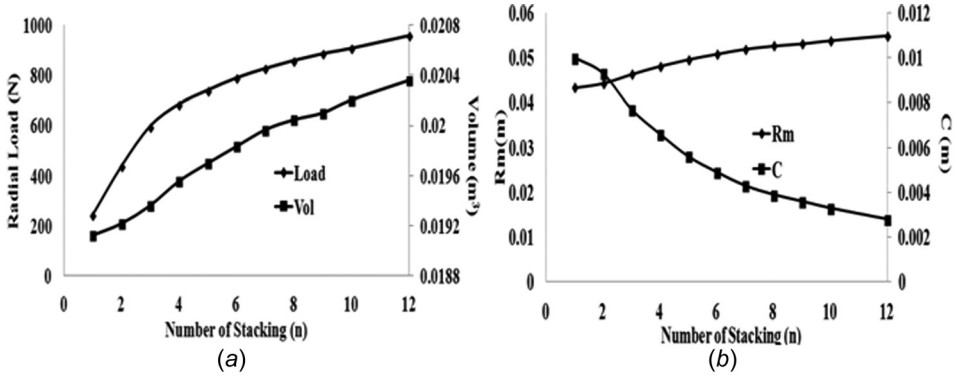

Fig. 4 Variation of parameters of conventional PMB with number of stacking: (*a*) no. of stacking versus load and volume and (*b*) no. of stacking versus R_m and C

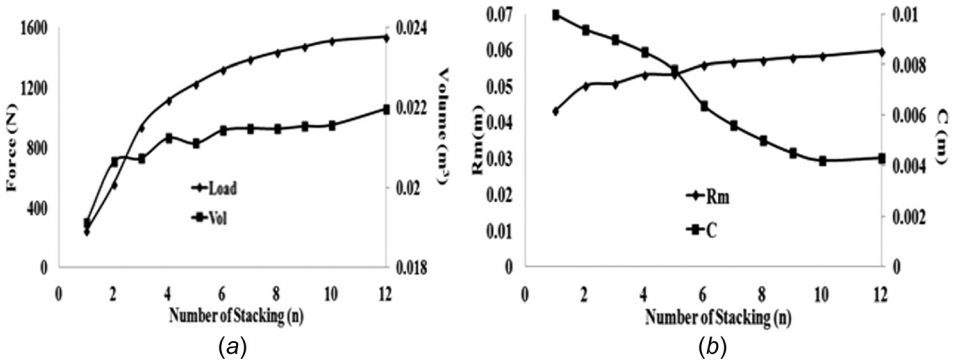

Fig. 5 Variation of parameters of RMD configured PMB with number of stacking: (*a*) no. of stacking versus load and volume and (*b*) no. of stacking versus R_m and C

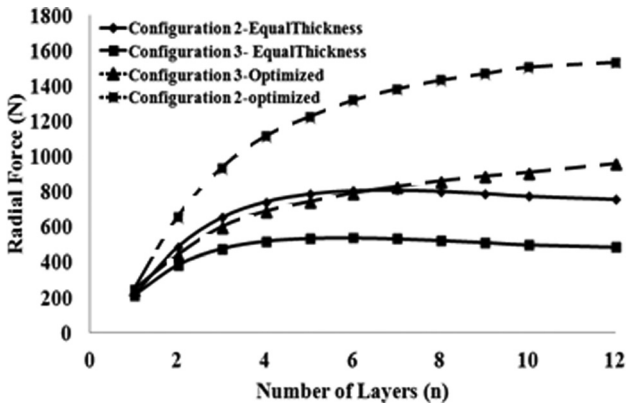

Fig. 6 Radial force as a function of number of layers for configurations 2 and 3 having same radial thickness of rotor and stator magnets and optimization results

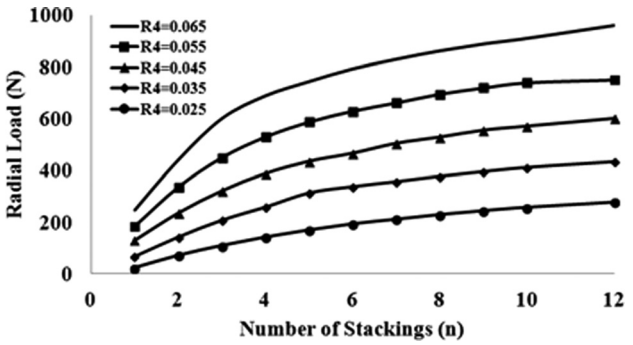

Fig. 8 Radial load versus number of stacking for different outer radius values in configuration 2

numbers of stacking is plotted in Fig. 8 and the obtained R_m and C values with respect to L are presented in Figs. 9(*a*) and 9(*b*), respectively. The equation representing the variation of R_L and R_C with respect to R_4 is given in Eqs. (12) and (13), respectively. The estimated values using these equations along with values obtained from optimization are plotted in Fig. 10. From this figure, it can be noted that these equations can be used precisely in estimating the values obtained from optimization

$$R_L = (0.029\ L^{-1.12})\,(0.065/R_4) \tag{12}$$

$$R_C = (0.024\ L^{-1.21} + 3.14)(0.065/R_4) \tag{13}$$

The above procedure is adopted for determining the equations for R_C, R_L, and load for configuration 3. The value of optimum force with respect to stacking length for different values of R_4 is plotted in Fig. 11. The obtained values of R_L and R_C for different L and $R_4 = 0.065$ values are plotted in Figs. 12(*a*) and 12(*b*), respectively. From these figures, it can be observed that trend of R_L and R_C values with respect to L for configuration 3 is same as in configuration 2. The proposed modified equations are given by

$$R_L = (0.0355\ L^{-1.095}) \tag{14}$$

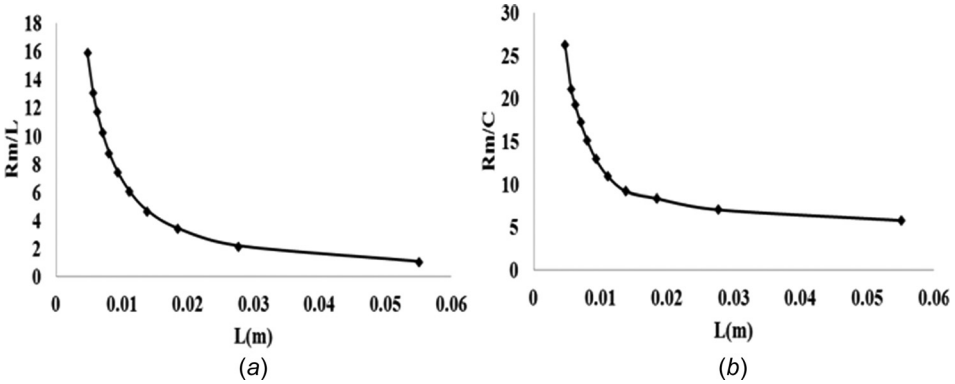

Fig. 7 Variation of R_L and R_C with respect to L for configuration 2: (*a*) R_L versus L and (*b*) R_C versus L

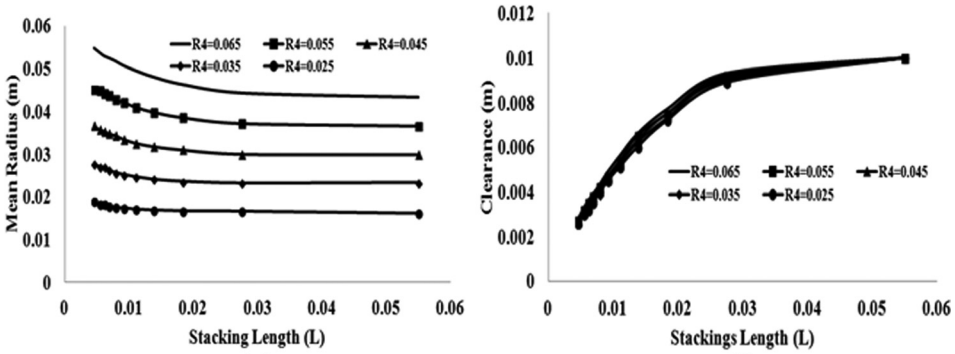

(*a*) (*b*)

Fig. 9 Variation of R_L and R_C with respect to L in configuration 2: (*a*) R_m versus L and (*b*) C versus L

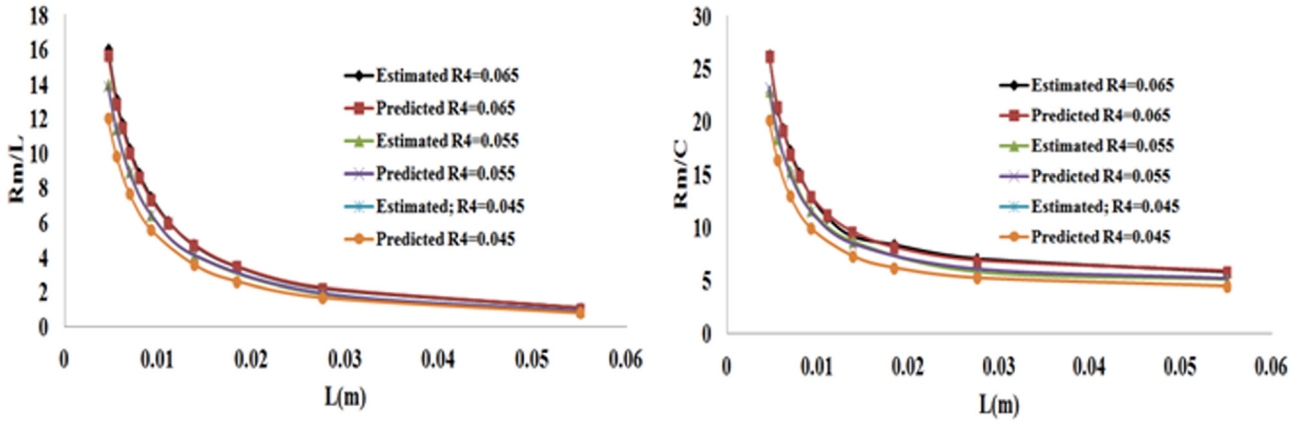

(*a*) (*b*)

Fig. 10 Estimated and predicted values of R_L and R_C for different values of $R_4 = 0.065$ m, 0.055 m, and 0.045 m for configuration 2: (*a*) R_L versus L and (*b*) R_C versus L

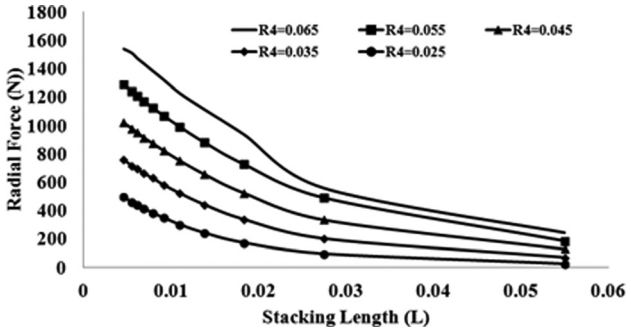

Fig. 11 Radial load versus number of stacking for different outer radius values for configuration 3

$$R_C = (0.0225\ L^{-1.17} + 3.4) \tag{15}$$

Final form of R_L and R_C equations with varying R_4 is presented in Eqs. (16) and (17). The values of R_L and R_C estimated from the optimization and from Eqs. (16) and (17) are plotted in Fig. 13. From these figures, it is clearly evident that these equations are capable of predicting optimization values very accurately and precisely

$$R_L = (0.0355\ L^{-1.095})(0.065/R_4) \tag{16}$$

$$R_C = (0.0225\ L^{-1.17} + 3.4)(0.065/R_4) \tag{17}$$

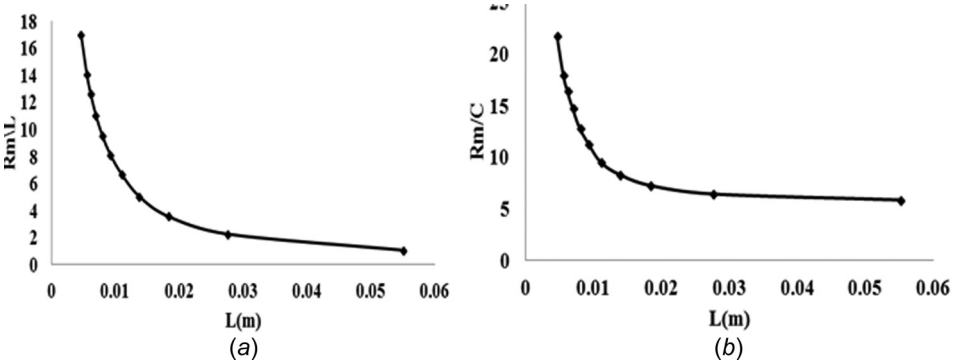

(*a*) (*b*)

Fig. 12 Variation of R_L and R_C with respect to L for configuration 3: (*a*) R_L versus L and (*b*) R_C versus L

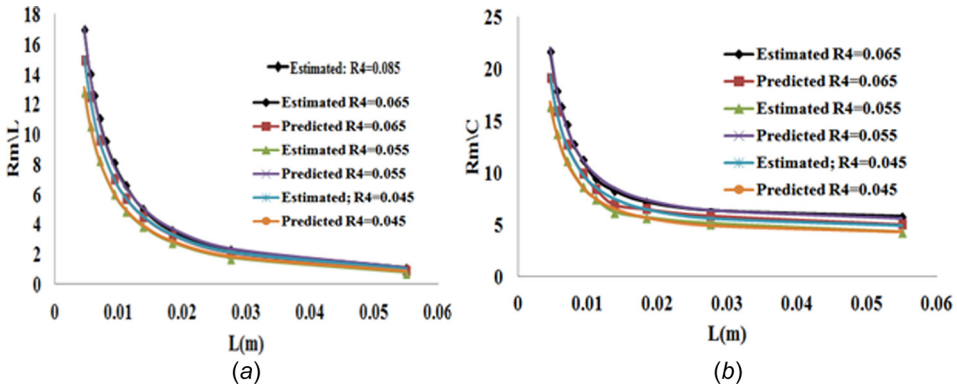

Fig. 13 Estimated and predicted values of R_L and R_C with respect to L for configuration 3 and for different values of R_4: (a) R_L versus L and (b) R_C versus L

Table 4 Dimensions of PMBs considered for validation

Case	References	Dimensions of the PMB				
		R_1 (m)	R_2 (m)	R_3 (m)	R_4 (m)	H (m)
1	[18]	0.011	0.02	0.0245	0.0375	0.05
2	[6]	0.01	0.02	0.022	0.032	0.05
3	[16]	0.005	0.024	0.025	0.035	0.05

Application of the Proposed Model

Validation of the proposed equations is carried out using three bearing dimensions extracted from the available published literature [6,15,17]. Bearing dimensions from these literatures are tabulated in Table 4.

Stepwise procedure to be followed in estimating the load for different stacking configurations is as follows:

(i) Calculate the value of R_m for different configurations from the equation provided for R_L ($R_m = LR_L$). For configuration 2, use Eq. (12) and for configuration 3 use Eq. (16). For configuration 1, either of these equations can be used.

(ii) Similarly, the value of C for different configurations is determined from R_C value which is determined from Eq.

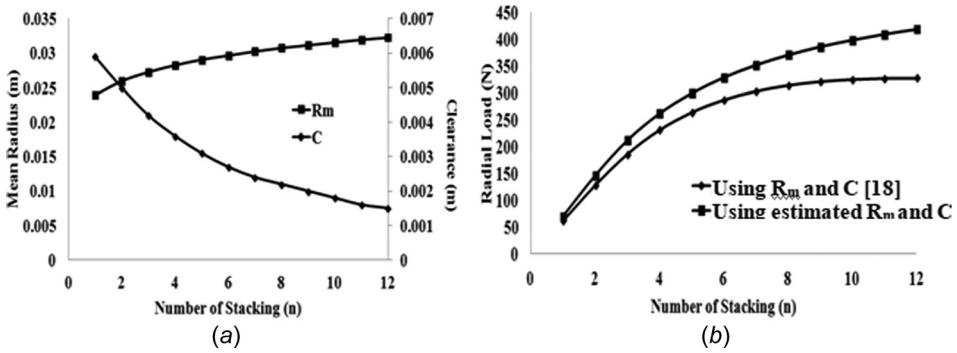

Fig. 14 Estimated values of R_m and C and comparison of loads obtained from dimension from Ref. [17] and for estimated R_m and C, for configuration 2: (a) R_m and C values with respect to n and (b) load versus n

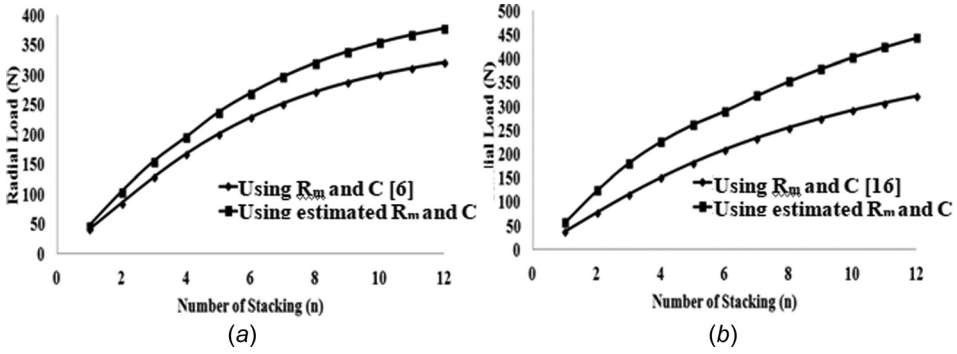

Fig. 15 Comparison of loads obtained for dimension provided in literatures and for estimated R_m and C: for case 2 (a) [6] and case 3 (b) [15], for configuration 2

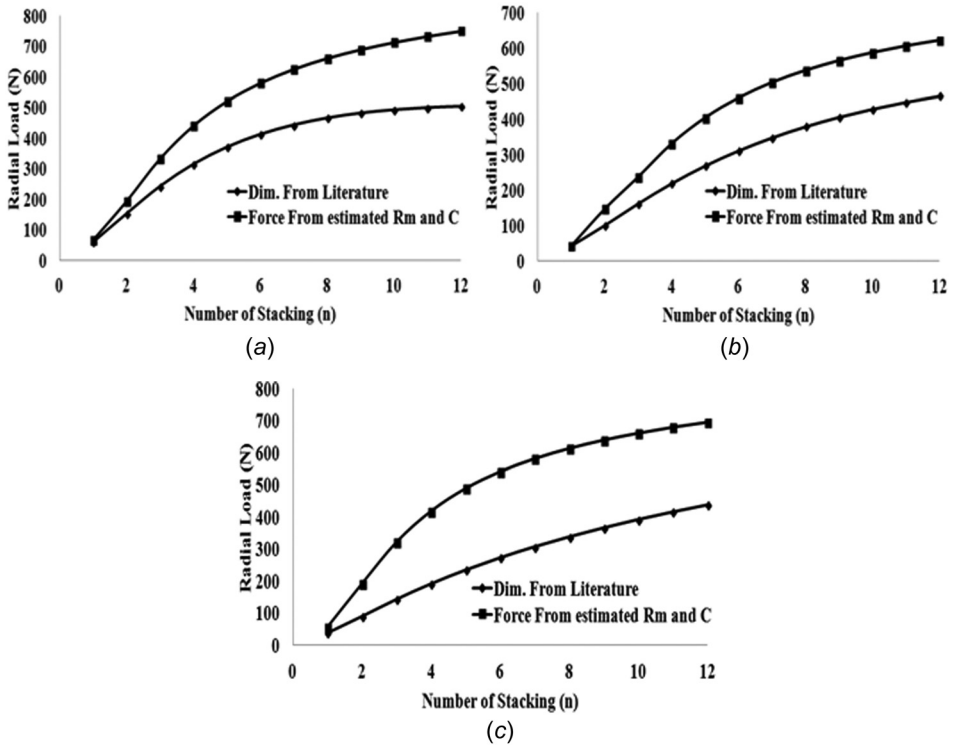

Fig. 16 Comparison of loads obtained for dimensions provided in literatures and estimated R_m and C: for cases 1–3, for configuration 3. (*a*) Case 1, (*b*) case 2, and (*c*) case 3.

(13) for configuration 2 and for configuration 3, Eq. (17) has to be utilized. For configuration 1, either of these equations can be used.

(iii) From optimization, it could be observed that irrespective of the bound values of R_1 (0.002–0.022), the optimum value tends to be on the lower side. Therefore, the values of R_1 presented in the literature will be considered for optimization.

(iv) For the obtained R_m and C values, the radial load for configurations 1, 2, and 3 is calculated from Eqs. (1), (3), and (4), respectively.

For case 1, the obtained values of R_m and C for $R_1 = 0.011$ m, $R_4 = 0.0375$ m, $H = 0.05/n$, and n varying from 1 to 12 are plotted in Fig. 14(*a*). Estimated radial load for the aforementioned values of R_m and C as well as the values of R_m and C provided by Mystkowski and Ambroziak [17] is plotted in Fig. 14(*b*). Similarly, the load values for cases 2 and 3 are plotted in Figs. 15(*a*) and 15(*b*), respectively. From all these three cases, it is inferred that using the proposed equation of R_m and C, higher load-carrying capacity can be achieved.

To demonstrate the effectiveness of the proposed methodology, the results obtained from the proposed equation will be compared with the optimization equation provided by Moser et al. [8]. The steps to be followed for obtaining the optimum dimension of conventional stacked PMB are as follows:

Step 1: Determine the ratio of the C/R_4. The value of C/R_4 must be between 0.01 and 0.06

Step 2: Based on the value of C/R_4, the values of R_1/R_4, R_2/R_4 and L/R_4 is estimated using the graphs provided.

To obtain the dimension of stacked PMB using the equation provided by Moser et al. [8], the value of R_1/R_4, is estimated for all three cases. The calculated values of R_1/R_4 for all three cases are: 0.12, 0.0625, and 0.0285. Since the value of R_1/R_4 must be between 0.01 and 0.06, calculation is performed only for case 3. Using the graphs provided by Moser et al. [8], the calculated values of R_1, R_2, and L are 0.021, 0.028, and 0.0028, respectively. For this case, the estimated number of layer (n) is 18 and radial load is 414 N. It is worth noting that using the proposed equation, load-carrying capacity of 423 N is achieved for having $n = 11$. Hence, it can be concluded that the proposed equations are superior to the equation provided by Moser et al. [8].

Similarly, the plots obtained for configuration 3, for different cases: cases 1–3, are plotted in Figs. 16(*a*)–16(*c*), respectively. From this plot, it can be observed that the load-carrying capacity has enhanced by using the estimated R_m and C values from Eqs. (16) and (17). Hence, by using the estimated R_m and C values, an optimum load-carrying capacity can be achieved.

Conclusion

The pragmatic optimization of three different axially stacked PMB configurations for the maximum radial load was presented using 3D equations. The presented optimization is based on the constraints, constants, and bounds of the dimensions obtained from the data available in literatures. The proposed equations of mean radius and clearance for the given axial length and outer radius of the stator will assist the designer effectively in the development of stacked PMBs for higher load sustainability. To envisage the effictiveness of the proposed methodology, three dimensions of stacked PMB from literatures were considered. It was demonstrated that using the estimated R_m and C values, optimum load-carrying capacity can be achieved for a given dimension of stacked PMB. Further, it was demonstrated that the proposed equation is capable of predicting wide range of dimension and a superior results compared to the established equations.

Nomenclature

B = length of rotor magnet (m)
Br_1 = magnetic remanence of stator (T)
Br_2 = magnetic remanence of rotor (T)
C = radial clearance (m)
E = eccentricity (m)
$F_{y,a}$ = radial load exerted by single layer magnet (N)
$F_{y,CON}$ = radial load exerted by conventional stacked PMB (N)

$F_{y,\mathrm{RMD}}$ = radial load exerted by RMD configured PMB (N)
$F_{y,s}$ = radial force between two sector magnets (N)
H = length of stator (m)
L = axial length stacked ring (m)
N = number of stacking
r_{12}, r_{34} = position vector (m)
R_C = R_m/C
R_L = R_m/L
R_m = mean radius (m)
R_1 = inner radius of rotor magnet (m)
R_2 = outer radius of rotor magnet (m)
R_3 = inner radius of stator magnet (m)
R_4 = outer radius of stator magnet (m)
Vol = volume (m^3)
z_a = axial offset (m)
ε = eccentricity ratio
θ = angle subtend by rotor magnet (rad)
θ' = angle subtend by stator magnet (rad)
μ_0 = permeability of air

Suffices

a = monolayer magnet
CON = conventional
k = number of stacking of magnetic ring for RMD PMBs
m = number of stacking of magnetic ring for conventional PMBs
p = perpendicular
RMD = rotational magnetization direction
y = y direction

References

[1] Filion, G., Ruel, J., and Dubois, M., 2013, "Reduced-Friction Passive Magnetic Bearing: Innovative Design and Novel Characterization Technique," Machines, **1**(3), pp. 98–115.
[2] Morales, W., Fusaro, R., and Kascak, A., 2003, "Permanent Magnetic Bearing for Spacecraft Applications," Tribol. Trans., **46**(3), pp. 460–464.
[3] Mukhopadhyay, S. C., Ohji, T., and Iwahara, M., 2000, "Modeling and Control of a New Horizontal-Shaft Hybrid-Type Magnetic Bearing," IEEE Trans. Ind. Electron., **47**(1), pp. 100–108.
[4] Paden, B., Groom, N., and Antaki, J. F., 2003, "Design Formulas for Permanent-Magnet Bearings," ASME J. Mech. Des., **125**(4), pp. 734–738.
[5] Yonnet, J. P., Lemarquand, G., Hemmerlin, S., and Olivier Rulliere, E., 1991, "Stacked Structures of Passive Magnetic Bearings," J. Appl. Phys., **70**(10), pp. 6633–6635.
[6] Bekinal, S. I., and Jana, S., 2016, "Generalized Three-Dimensional Mathematical Models for Force and Stiffness in Axially, Radially, and Perpendicularly Magnetized Passive Magnetic Bearings With 'n' Number of Ring Pairs," ASME J. Tribol., **138**(3), p. 031105.
[7] Lijesh, K. P., and Hirani, H., 2015, "Development of Analytical Equations for Design and Optimization of Axially Polarized Radial Passive Magnetic Bearing," ASME J. Tribol., **137**(1), p. 011103.
[8] Moser, R., Sandtner, J., and Bleuler, H., 2006, "Optimization of Repulsive Passive Magnetic Bearings," IEEE Trans. Magn., **42**(8), pp. 2038–2042.
[9] Ravaud, R., Lemarquand, G., Lemarquand, V., and Depollier, C., 2009, "Calculation of the Magnetic Field Created by Permanent Magnets," Prog. Electromagn. Res. B, **11**, pp. 281–297.
[10] Van, B. M., Kluyskens, V., and Dehez, B., 2017, "Optimal Sizing and Comparison of Permanent Magnet Thrust Bearings," IEEE Trans. Magn., **53**(2), p. 8300110.
[11] Bekinal, S. I., Doddamani, M., and Jana, S., 2017, "Optimization of Axially Magnetized Stack Structured Permanent Magnet Thrust Bearing Using Three-Dimensional Mathematical Model," ASME J. Tribol., **139**(3), p. 031101.
[12] Ravaud, R., Lemarquand, G., and Lemarquand, V., 2009, "Force and Stiffness of Passive Magnetic Bearings Using Permanent Magnets—Part 1: Axial Magnetization," IEEE Trans. Magn., **45**(7), pp. 2996–3002.
[13] Lijesh, K. P., and Hirani, H., 2014, "Stiffness and Damping Coefficients for Rubber Mounted Hybrid Bearing," Lubr. Sci., **26**(5), pp. 301–314.
[14] Tan, Q., Li, W., and Liu, B., 2002, "Investigations on a Permanent Magnetic–Hydrodynamic Hybrid Journal Bearing," Tribol. Int., **35**(7), pp. 443–448.
[15] Samanta, P., and Hirani, H., 2008, "Magnetic Bearing Configurations: Theoretical and Experimental Studies," IEEE Trans. Magn., **44**(2), pp. 292–300.
[16] Lijesh, K. P., and Hirani, H., 2015, "Magnetic Bearing Using Rotation Magnetized Direction Configuration," ASME J. Tribol., **137**(4), p. 042201.
[17] Mystkowski, A., and Ambroziak, L., 1980, "Investigation of Passive Magnetic Bearing With Halbach-Array," Acta Mech. Autom., **4**(4), pp. 78–82.
[18] Fengxiang, W., Jiqiang, W., Zhiguo, K., and Fengge, Z., 2004, "Radial and Axial Force Calculation of BLDC Motor With Passive Magnetic Bearing," Forth International Power Electronics and Motion Control Conferences (IPEMC), Xi'an, China, Aug. 14–16, pp. 290–293.
[19] Lijesh, K. P., and Hirani, H., 2015, "Modeling and Development of RMD Configuration Magnetic Bearing," Tribol. Ind., **37**(2), pp. 225–235.
[20] Byrd, R. H., Jean, C. G., and Jorge, N., 2000, "A Trust Region Method Based on Interior Point Techniques for Nonlinear Programming," Math. Program., **89**(1), pp. 149–185.